

This is an Accepted Manuscript of an article published by Elsevier in Scripta Materialia, 69 (7), 529 – 532 on October 2013, available at: <https://doi.org/10.1016/j.scriptamat.2013.06.019> . It is deposited under the terms of the Creative Commons Attribution-NonCommercial-NoDerivatives License (<http://creativecommons.org/licenses/by-nc-nd/4.0/>), which permits non-commercial re-use, distribution, and reproduction in any medium, provided the original work is properly cited, and is not altered, transformed, or built upon in any way.

EVIDENCE OF NANO-GRAIN CLUSTER COALESCENCE IN SPARK PLASMA SINTERED α -Al₂O₃

A. Morales-Rodríguez^{a,*}, R. Poyato^b, A. Gallardo-López^a, A. Muñoz^a and A. Domínguez-Rodríguez^a

^a Department of Condensed Matter Physics, Universidad de Sevilla, BOX 1065, 41080 Sevilla, Spain

^b Materials Science Institute of Sevilla (CSIC-Universidad de Sevilla), Américo Vespucio 49, 41092 Sevilla, Spain

*Corresponding author. E-mail address: amr@us.es (A. Morales-Rodríguez)

The aim of this study is to elucidate the coarsening kinetics involved during densification of fine-grained pure α -alumina by spark plasma sintering. Low temperature and short dwell time sintering conditions were used to preserve the nanocrystalline structure of the starting commercial powder (about 50 nm). Notwithstanding the above, submicron grain coarsened microstructures have been developed. The microstructure evolution of alumina with different sintering conditions points to nano-grain rotation densification mechanism as responsible for the fast grain growth observed.

Keywords: spark plasma sintering; crystalline nanostructure; grain growth

The enhanced optical and mechanical properties exhibited by bulk fine-grained alumina [1-2] encourage the scientific community to direct their efforts to obtain fully dense nanocrystalline alumina. The goal in nanoceramic sintering is to get full-density while maintaining the grain size below 100 nm [3]. Conventional sintering techniques involve long heating periods up to sintering temperatures that unavoidably promote significant grain growth. Nowadays, fast sintering seems to be a promising method to achieve this challenge overcoming the grain growth promoted at the final stages of conventional sintering [3]. The spark plasma sintering (SPS) is a high heating rate technique that allows rapid densification limiting grain growth by lattice or grain boundary diffusion [4]. In this method, the simultaneous application of pressure and electrical pulsed current through the sample during heating allows fast densification of ceramics at relatively low temperatures and pressures. In order to achieve the maximal densification while avoiding exaggerated grain growth, careful attention must be paid to the sintering time and temperature [5-7].

In recent years, several works were devoted to the study of SPS processing of α -Al₂O₃. Systematic studies of the effect of the SPS parameters on densification and grain growth have been carried out for pure and doped α -Al₂O₃ [6-9] and fine-grained microstructures have been reported. Shen et al. [7] reported a study of the effect of SPS parameters on densification and grain growth of alumina powder with 0.4 μ m particle

size, and obtained fully dense ceramics with submicrometric grain size (0.6 μm). A lower grain size (300 nm) and full densification was obtained by Santanach et al. after SPS of alumina powder with 140 nm particle size at 1200°C for 3 minutes or 1100°C for 15 minutes [9].

Up to our knowledge only the works of Mishra and Mukherjee [10] and Zhan et al. [5,11] have performed spark plasma sintering of $\alpha\text{-Al}_2\text{O}_3$ powders with average particle size of 50 nm. Although dense aluminas were obtained in these works, the powder nanostructure was not retained. After SPS at 1300°C for 8 minutes materials with 98.2% relative density and submicrocrystalline structure (0.7 μm) were obtained [10]. By cold-pressing at 200 MPa before SPS, Zhan et al. [5,11] achieved dense $\alpha\text{-Al}_2\text{O}_3$ at sintering temperature as low as 1150°C for only 3 min with an important grain refinement (final grain size of about 350 nm) that unfortunately was not enough to preserve the nanocrystalline powder character.

Despite the complete and detailed studies on processing and microstructure carried out by different authors, the mechanisms controlling densification and grain growth in alumina are still matter of debate. In this context, the present work is devoted to carefully analyze the microstructure evolution of nano α -alumina powder sintered by SPS under different temperature and dwell time conditions to elucidate the grain growth kinetics involved during densification.

Commercial nanocrystalline $\alpha\text{-Al}_2\text{O}_3$ powder (Nanostructured & Amorphous Materials, Inc., Houston, USA), with 99% purity, nearly spherical particle shape and particle diameter ranging from 30 to 40 nm was used. Samples of 15 mm in diameter and 2-3 mm in thickness were sintered using a SPS equipment (model 515S, SPS Dr. Sinter Inc., Kanagawa, Japan) operating under vacuum with uniaxial pressure applied at room temperature and held constant until the end of the sintering dwell time. Different pressure (75 and 100 MPa), temperature (1200, 1250 and 1300°C) and holding time (5, 10, 15 and 30 min) sintering conditions were selected to study the influence of these parameters on the densification process and grain coarsening. In order to obtain a rough comparison between grain growth promoted in conventional furnaces and in SPS process, the sample sintered at 1300°C for 30 minutes was compared with another one sintered for 5 minutes and thermally treated in air at 1300°C for 30 minutes.

The final density of the as-sintered samples was measured by the Archimedes method with distilled water as immersion medium and was referred to the theoretical density of 3.98 $\text{g}\cdot\text{cm}^{-3}$ for alumina. Phase identification was carried out using x ray diffraction (XRD, model D8 Advance A25, Bruker Co., Massachusetts, USA). The Rietveld method was used for quantitative texture analysis and LeBail fitting of the spectra data was performed to evaluate residual strains of dense materials.

Transversal cross sections of samples were mechanical ground and diamond polished down to 1 μm . Thermal etching of polished samples was conducted in air atmosphere at 100°C below each sintering temperature for 15 min to reveal the grain microstructure. Thermally etched polished surfaces were observed in a high-resolution scanning electron microscope (HRSEM) (Hitachi S5200, Hitachi High Technologies America Inc., USA). Transmission electron microscopy (TEM) samples were prepared by conventional procedure of mechanical thinning, dimpling and ion milling over a material foil, and examined using a Hitachi H800 electron microscope. The

microstructure analysis was performed on HRSEM micrographs. Characterization of the grain morphology has been made measuring about 300 grains to obtain the equivalent planar diameter, $d = 2(\text{area}/\pi)^{1/2}$, as grain size parameter (mean, standard deviation, mode, median and maximum values have been evaluated to characterize the grain size distribution) and the shape factor, $F = (4\pi \cdot \text{area})/(\text{perimeter})^2$.

Table 1 displays the sintering conditions, density and morphological parameters of the different $\alpha\text{-Al}_2\text{O}_3$ samples. For sintering temperatures below 1300°C, dense materials have not been produced. Increasing the dwell time or the sintering temperature have shown similar effects by increasing densification and final grain size. The materials with similar low relative densities exhibited similar mean grain size regardless the sintering time: about 100 nm for $\rho < 80\%$ and 300 nm for $90\% < \rho < 95\%$. On the contrary, a noticeable effect of sintering time on final grain size is observed when relative densities are up to 98%. Estimated grain sizes over 700 nm are in agreement with the observations made in ultrafine grained alumina prepared under similar sintering conditions by Mishra and Mukherjee [10]. The as-sintered microstructure consists of elongated alumina grains that tend to be aligned in direction perpendicular to pressure axis (see fig. 1); most of them present a mean shape factor close to 0.7 (table 1) whereas a few percent (< 5%) exhibits very acicular shapes with F value close to 0.

All as-sintered specimens exhibited Gumbel grain size distribution with abnormally wide standard deviations close to 2/3 of the mean grain size value. This could be related to a non-equilibrium grain configuration attained after SPS process, since after annealing at 1300°C for 30 min the grain population exhibited better fit to lognormal distributions usually assumed for grain growth analysis in ceramics [12].

Results presented in table 1 show that, although low sintering temperature and short dwell time have been used in order to retain the nanostructure of the starting powder, dense nanostructured aluminas were not obtained. Even materials with densities below 80% increased their grain size by a factor between 2 and 2.5 the size of the starting powder, which indicates that grain growth occurs very fast at temperatures as low as 1200°C. In addition, annealing of dense alumina in conventional furnace at 1300°C for 30 min has shown that promoted grain growth with this slow heating procedure (780 nm mean grain size in alumina after annealing) was less noticeable than the one observed after spark plasma sintering of alumina under similar temperature and dwell time conditions (960 nm mean grain size, see table 1).

XRD diffraction patterns confirmed that both commercial alumina powder and sintered alumina contain only corundum α -phase. Rietveld analysis of X-ray diffraction data pointed out that preferred crystallographic orientation changes from expected $\{1\ 0\ -1\ 4\}$ plane found in the starting powder (14 vol.%) to $\{0\ 3\ -3\ 0\}$ plane in case of dense aluminas sintered at 1300°C. The role of the SPS process on the reorientation to $\{0\ 3\ -3\ 0\}$ plane could be related to the fact that sintering under pressure may facilitate the piling-up of these hexagonal crystals with c-axis perpendicular to the loading direction. Increasing dwell time at 1300°C significantly reduces the effect of texture from 29 vol.% crystals oriented in the ceramic sintered for 5 min, to 20 vol.% and 14 vol.% in the ceramics sintered for 10 and 30 min respectively. Small residual strains of 1.0 and 1.2% have been estimated in the aluminas sintered for 5 and 30 min respectively, whereas no strain has been

measured in the starting powder and in the alumina sintered for 10 min at 1300°C. These differences observed in preferred orientation and strain promoted by SPS in these materials must be taken into account when assessing their mechanical properties. For instance, Álvarez-Clemares et al. [13] have recently published that residual strain introduced in alumina as consequence of the SPS process concentrates at grain boundaries and acts as crack propagation inhibitor improving flexural strength and fracture toughness.

HRSEM images show the typical microstructure developed after SPS process (Fig. 1). Grain population of the samples exhibits abnormal grain growth and nanometric multigrain clusters are usually observed inside the abnormal grains. This microstructure of nano-grain clusters visible within the larger grains has been previously reported in yttrium aluminum garnet $Y_3Al_5O_{12}$ (YAG) prepared by SPS from nanocrystalline particles of 34 nm [14]. Aggregate type morphology inside large grains has also been observed in a pressure-less spark plasma sintered alumina [15]. These clusters did not exhibit nanocrystalline character [15].

Under different temperature conditions the number of revealed grains forming the cluster inside larger grains changes. At lower sintering temperature many grains seem to be the result of assembling the powder particles (Fig. 2A) whereas a dramatic reduction in the cluster size, i.e. the number of grains in the cluster, is observed with increasing temperature (Fig. 2B). A similar evolution in the cluster nanostructure has been found with increasing dwell time at low temperature (30 min at 1200°C), as shown in figure 1, although the cluster size reduction is less remarkable. The cluster's grains have a mean grain size close to the starting powder particle size (70 nm) and rounded shape ($F = 0.79$). This nanocluster structure was preserved after post-sintering thermal treatment (image not shown).

The nature of grain boundaries inside clusters has been studied by TEM. Figure 3 shows arrays of dislocations pointing out that the clusters consist of subgrains separated by low angle grain boundaries (LAGBs). Some residual pores are also observed, the ones showing a round shape present high coordination number while the elongated ones exhibit lower coordination number. During densification of nanocrystalline YAG powder by SPS, the formation of LAGBs starting from coupled rotation of nanocrystalline grains with high-angle grain boundaries (HAGBs) have been related to grain growth through grain rotation mechanism [14].

Although the uniaxial pressures of 75 and 100 MPa used in this study could be high enough to enable instantaneous densification via plastic deformation at the initial sintering stages according to [16], we assume that this is not the dominant mechanism because resistance to plastic deformation in alumina persists to high temperatures ($> 0.5T_m$) and it should result in specimens consisting of grains of approximately the same size as the corresponding initial powders as found by Meng et al. [17]. In oxides vulnerable to plastic deformation at lower temperatures, a lack of significant grain growth has also been observed after SPS as in the case of fully dense nanocrystalline MgO specimens [18-19].

Conversely, the formation of these multigrain clusters with internal LAGBs suggests that densification and grain growth from α -alumina nano-powder take place mainly by grain rotation and sliding mechanism similarly to YAG nano-powder spark plasma

sintered [14,20]. The rounded shape observed in cluster's grains (see fig. 1) could favor grain rotation via viscous process without the need for other accommodation mechanism and small residual pores observed by TEM (see fig. 3) would arise from such nano-grain rotations. Salamon and Shen [15] reported enormous grain growth in α -Al₂O₃ with the formation of cluster structures using a starting powder of 100 nm and they also suggested that coarsening probably took place via particle sliding and rotation mechanism in their pressure-less spark plasma sintered alumina.

Recently, a new model of grain coalescence by grain rotation in nano-ceramics developed by R. Chaim [21] proposed that hard elastic nano-particles may rotate and slide to form low-energy LAGBs. This leads to grain coalescence much faster than by normal grain growth even without applying external pressure. According to this, the grain rotation mechanism may also be active from the initial heating stage of the sintering process and the ability for nano-grain rotation strongly depends on the inverse of grain size being greater the smaller the particle size. The model adequately explains the formation of small grain clusters observed in this study in the case of high-dense aluminas and the fast grain growth observed at low densities and temperatures as low as 1200°C.

Previous discussion points out the nanometric character of the starting particle size as responsible for impeding the nanostructure consolidation to sizes below 100 nm by spark plasma sintering of α -alumina using pressure conditions below yield point value. In this case, the results presented in this paper suggest that grain coalescence by nano-particles rotation and sliding is strongly favored.

The authors would like to acknowledge the financial support awarded by the Spanish Ministry of Science and Innovation through the project MAT2009-11078. Microscopy studies have been performed in facilities belonging to the Microscopy Service (CITIUS, Universidad de Sevilla). They are also grateful to Dr. Santiago Medina Carrasco for his help and advice in the analysis of XRD data (X-Ray Laboratory, CITIUS, Universidad de Sevilla).

- [1] B.N. Kim, K. Hiraga, K. Morita, H. Yoshida, *Scripta Mater.* 57 (2007) 607.
- [2] A. Krell, P. Blank, *J. Am. Ceram. Soc.* 78 (1995) 1118.
- [3] K. Lu, *Int. Mater. Rev.* 53 (2008) 21.
- [4] Z.A. Munir, U. Anselmi-Tamburini, M. Ohyanagi, *J. Mater. Sci.* 41 (2006) 763.
- [5] G.D. Zhan, J. Kuntz, J. Wan, J. Garay, A.K. Mukherjee, *Scripta Mater.* 47 (2002) 737.
- [6] S.H. Risbud, C.H. Shan, A.K. Mukherjee, M.J. Kim, J.S. Bow, R.A. Holl, *J. Mater. Res.* 10 (1995) 237
- [7] Z. Shen, M. Johnsson, Z. Zhao, M. Nygren, *J. Am. Ceram. Soc.* 85 (2002) 1921.
- [8] G. Bernard-Granger, C. Guizard, *Acta Mater.* 56 (2008) 6273.
- [9] J.G. Santanach, A. Weibel, C. Estournès, Q. Yang, C. Laurent, A. Peigney, *Acta Mater.* 59 (2011) 1400.
- [10] R.S. Mishra, A.K. Mukherjee, *Mater. Sci. Eng. A* 287 (2000) 178.
- [11] G.D. Zhan, J. Kuntz, J. Wan, J. Garay, A.K. Mukherjee, *Mater. Sci. Eng. A* 356 (2003) 443.
- [12] S.K. Kurtz, F.M.A. Carpay, *J. Appl. Phys.* 51 (1980) 5725.
- [13] I. Álvarez-Clemares, A. Borrell, S. Agouram, R. Torrecillas, A. Fernández, *Scripta Mater.* 68 (2013) 603.

- [14] R. Chaim, Mater. Sci. Eng. A 443 (2007) 25.
- [15] D. Salamon, Z. Shen, Mater. Sci. Eng. A 475 (2008) 105.
- [16] Y. Aman, V. Garnier, E. Djurado, J. Am. Ceram. Soc. 94 (2011) 2825.
- [17] F. Meng, Z. Fu, J. Zhang, H. Wang, W. Wang, Y. Wang, Q. Zhang, J. Am. Ceram. Soc. 90 (2007) 1262.
- [18] R. Chaim, Z. Shen, M. Nygren, J. Mater. Res. 19 (2004) 2527.
- [19] A. Domínguez-Rodríguez, D. Gómez-García, E. Zapata-Solvas, Z. Shen, R. Chaim, Scripta Mater. 56 (2007) 89.
- [20] R. Chaim, J. Mater. Sci. 41 (2006) 7862.
- [21] R. Chaim, Scripta Mater. 66 (2012) 269.

TABLE TITLE

Table 1. Temperature, pressure and sintering time conditions selected for the different samples obtained by spark plasma sintering. Final density, mean grain size along with their standard deviation values and shape factor of the majority of the grain population (percentages are shown in parentheses) are also included.

T (°C)	P (MPa)	t (min)	ρ (%)	$\langle d \rangle$ (nm)	s.d. (nm)	F (% of grains)
1200	100	5	74	130	90	0.73 (99.9%)
		10	79	100	70	0.74 (95.8%)
		30	95	330	230	0.70 (99.4%)
1250	100	10	93	290	210	0.70 (100%)
	100	15	95	310	220	0.70 (99.2%)
1300	75	10	92	350	240	0.73 (95.5%)
	75	5	98	670	570	0.69 (99.1%)
		10	100	840	600	0.70 (99.3%)
30		98	960	760	0.67 (97.2%)	

FIGURE CAPTIONS

Fig.1. Detail of typical cluster size observed by HRSEM in alumina spark plasma sintered for 30 min at 1200°C. Pressure axis is indicated by arrows.

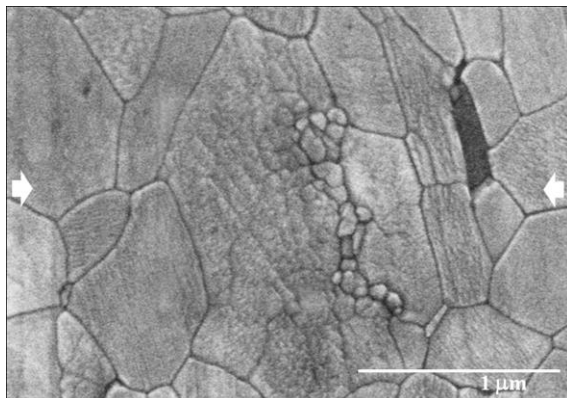


Fig.2. HRSEM micrographs of materials sintered for 5 min at (A) 1200°C and (B) 1300°C. Pressure axis is indicated by arrows.

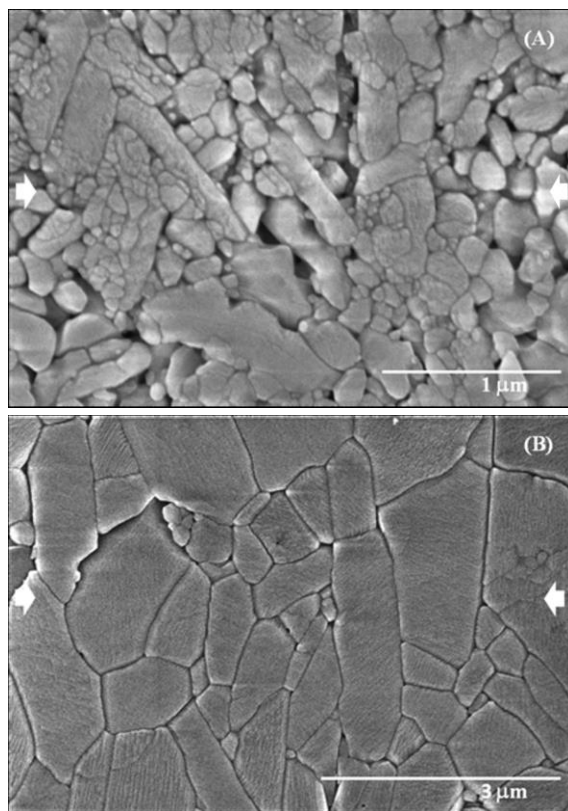


Fig.3. LAGBs structure of nanoclusters observed by TEM in alumina sintered at 100 MPa for 30 min at 1200°C. Several LAGBs are indicated by arrows.

